JOURNAL OF MATERIALS SCIENCE 16 (1981) 3381–3392

Strain concentration at the crack corners in polyethylene films*

G. ZAMFIROVA-IVANOVA†, M. RAAB, Z. PELZBAUER
Institute of Macromolecular Chemistry, Czechoslovak Academy of Sciences, 162 06 Prague 6, Czechoslovakia

The crack growth kinetics in blown low-density polyethylene film have been examined. It has been proposed from mechanical measurements that a zone of plastic deformation ahead of the crack tip acts as an obstacle to crack propagation, especially when the crack grows perpendicularly to the machine direction of the film. The existence and size of such a plastic zone have been revealed using a special microscopical method.

1. Introduction

Stress concentration around holes in a perfectly elastic continuum is predicted by the classical theory of elasticity. A material which exhibits plastic deformation cannot, however, transfer stresses higher than its upper yield stress. In such a material the stress peaks at the crack roots are lower than those in a perfectly elastic body. In many polymeric materials with high extensibility a change in the geometric shape of the crack also plays a role irrespective of the cause of this change (cold drawing or rubber-like elasticity). The deformational blunting of the crack tip and orientational strengthening of the polymeric material ahead of the crack reduces the severity of the crack and counteracts its further propagation. These protective mechanisms may even cause the time-to-break of the body to increase with increasing external stress during a certain stress interval. We have described [1–4] an anomalous maximum for the time-to-break dependence on stress of hydrophilic gels and a polyethylene film. A necessary condition for the occurrence of such a maximum consists in the existence of macroscopic defects artificially introduced into test pieces. On the other hand, however, such an anomalous maximum does not appear if the defects are too large, thus impeding the development of a more pronounced deformation of the whole body. Therefore, we ascribed the occurrence of the maximum to the above mentioned strain barrier at the root of a growing crack. Direct experimental evaluation of the strain field in the vicinity of a crack in a polyethylene film is presented in this communication.

2. Experimental details

2.1. Material and test pieces

Low-density polyethylene Unifos DFDS 6600 in the form of an extruded and blown film, approximately 60 μm thick, was used as the experimental material. The film was extruded by a Swedish manufacturer Celloplast AB (Norrköping) on a so-called adiabatic extruder, produced by Reifenhäuser. The following characteristics of the material are given by the manufacturer: Melt index MI = 0.3 g per 10 min, density $\rho = 0.922\,\mathrm{g\,cm^{-3}}$, number and mass average molecular masses determined by gel permeation chromatography $\bar{M}_{n_{GPC}} = 22 \times 10^3$, $\bar{M}_{w_{GPC}} = 250 \times 10^3$, degree of branching (long branches) determined according to Drotts $\Lambda_D = 2.5 \times 10^{-4}$. The blown film process has introduced a biaxial orientation into the film. For this reason, the properties of the film were characterized in two directions, namely, in the axial (machine) direction and in the transverse (cross) direction (Fig. 1). Test pieces in the form of strips were cut from the film in these two directions (Fig. 2), their width being 10 mm and gauge length 25 mm. In the centre of one edge the test pieces were provided with a side incision,

*Partly presented at the Eighth International Conference on Rheology, Naples, Italy, September 1–5, 1980.
†Present address: Krum Popov Street 76, Sofia-21, Bulgaria.

0022–2461/81/123381–12$03.20/0

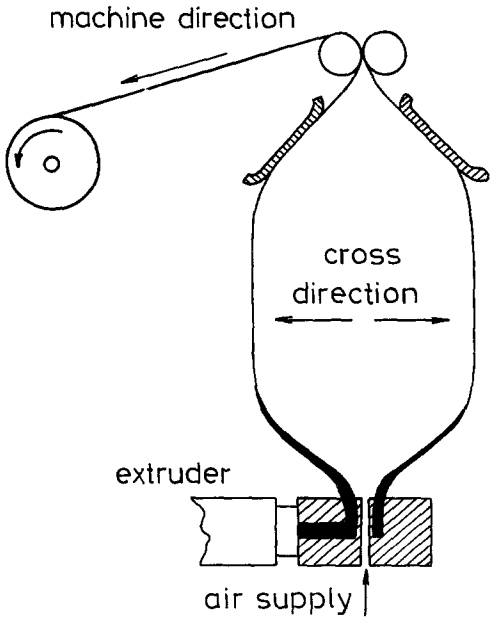

Figure 1 Scheme of the blown film process with the main directions of orientation indicated.

0.20 ± 0.02 mm long. The incisions were made with a razor blade using a simple device (Fig. 3), and their actual length was checked with a comparator.

2.2. Loading procedure and microscopic techniques

One part of the test piece was subjected to a constant load with simultaneous recording of the whole creep curve, while the other was deformed at constant speed using an Instron mechanical testing machine. In some selected cases the strain field near the crack propagating during the creep test was visualized by using a method suggested by one of the authors [5, 6]: Prior to straining, the surface of the sample was vacuum-coated with a brittle layer of carbon or aluminium; after deformation of the polymeric support this layer cracks, thus making it possible to determine the local strain. Even an aluminium film may be regarded as brittle because its elongation is approximately 150 times lower than that of the supporting polyethylene film. The layer is so thin (less than 0.1 μm) that its effect on the mechanical behaviour of the film can be neglected. For the purposes of this study, an aluminium layer was employed and the method was improved by using a clamp (Fig. 4) allowing the surroundings of the crack tip to be fixed at a given stage of its development, or at a chosen point of the creep curve. The region of

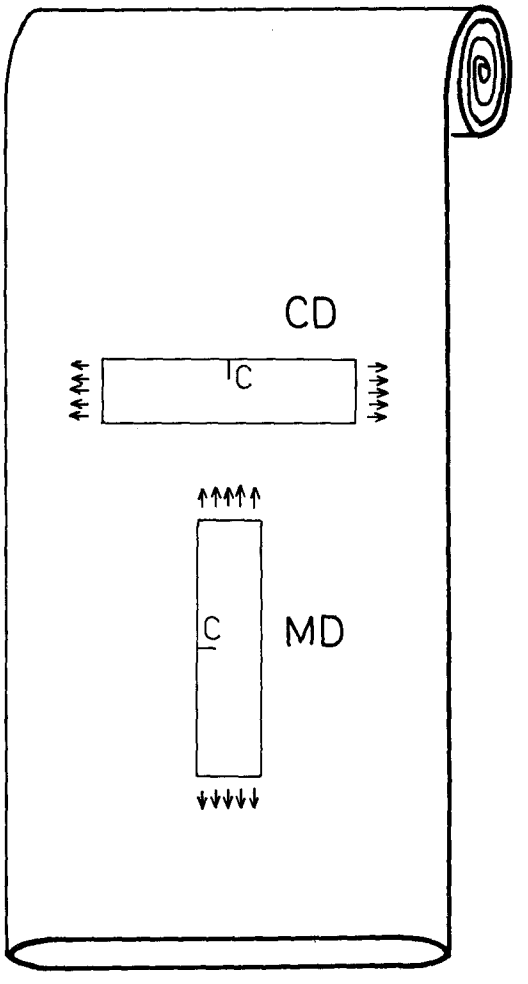

Figure 2 Scheme of test piece sampling from blow tubing film in both main directions.

the crack tip was then photographed in the transmitted light, both in the fixed state and after the clamp had been released. The microscope used was a Zetopan optical microscope manufactured by Reichert, Austria; the magnification on the negative was 14.4 times. The crack propagation in the regime of constant cross-head displacement rate in the Instron apparatus was observed only visually. After the test was interrupted at a chosen point of the stress–strain curve, the test piece was released from the jaws of the tensile-testing machine, and the crack length was measured with a comparator. For each measurement a new virgin sample was used. The cross-head speed used in the experiment was 2 cm min^{-1}.

3. Results and discussion

3.1. Crack propagation at constant load

The anisotropy of a biaxially oriented film is

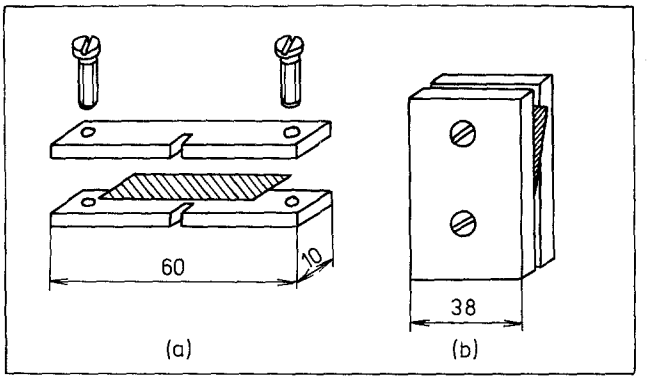

Figure 3 Master form (a) for cutting of test pieces and (b) device for fixation of the razor blade.

reflected not only in basic mechanical properties, such as the modulus of elasticity, yield stress and tensile strength: still more pronounced differences are observed in the resistance against crack propagation and also in the crack propagation kinetics. In this case, it seems that not only does anisotropy of the material properties in the bulk play a role, but in particular the ordered system of microstructural defects of elongated shape [7] or fissures becomes operative and either facilitates the propagation of the macroscopic crack (if parallel with the latter), or on the contrary hinders its propagation by interacting with the tip of the magistral crack (if oriented perpendicularly to its axis) [4]. In Fig. 5 the dependence of time-to-break on the stress for the test pieces with various edge-notch sizes is presented. The most striking features of this figure are the maxima which appear on the curves for test pieces cut in the cross direction and having artificial incisions 0.2 and 0.3 mm long. This means that within a narrow interval, the time-to-break increases with increasing external stress, contrary to expectation. In our preceding communication the occurrence of such an anomalous maximum was assigned to the orientational strengthening at the crack peaks [4]. A characteristic feature of the time-to-break maximum is also its statistical character. Experimental scatter is considerable in time-to-break measurements in general, but becomes especially large just in the range of the maximum. Actually, only part of the test piece exhibits a high time-to-break in this range, while the other part breaks after a much shorter time. The curve with the maximum then corresponds to an average of these two cases. It was shown experimentally [4] that the higher time-to-break values in the range of the maximum corresponded to creep curves with three inflection points. This suggests the existence of mechanisms impeding the propagation of an already proceeding crack. Such a view is corroborated by direct microscopic investigation of the crack geometry,

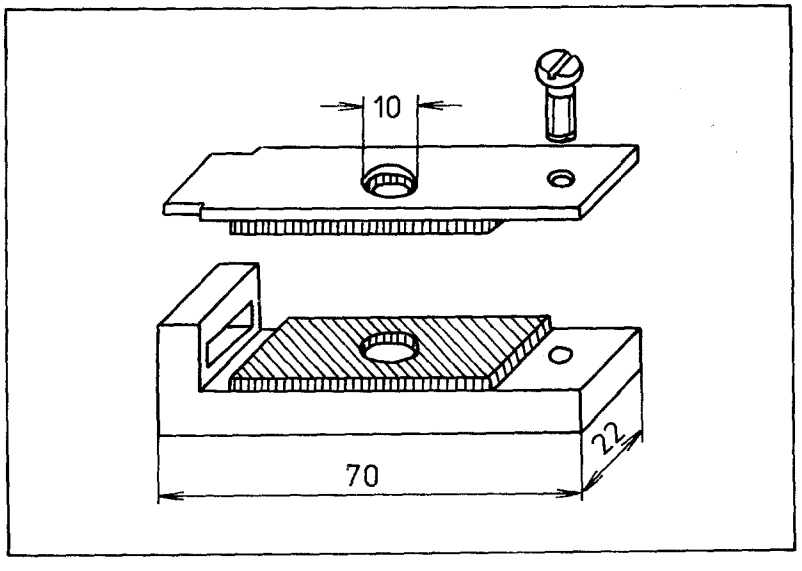

Figure 4 Clamp for fixation of crack surroundings in the stressed state.

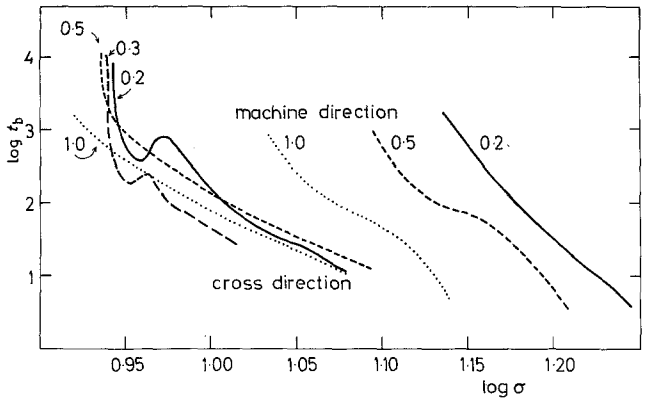

Figure 5 Dependence of the logarithm of time-to-break, log t_b, on the stress logarithm log σ for test pieces parallel and perpendicular to the machine direction of the film. The numbers indicate the initial incision length c_0 in mm. Note anomalous maxima for test pieces in cross direction with the smallest defects used.

and especially of the topography of the strain field in this work.

The crack propagation was examined microscopically on test pieces cut both in the axial and the transverse directions from the tubular film. Initial one-side incisions, $c_0 = 0.2$ mm long, were then introduced into all test pieces. The external stress related to the initial cross-section was 14.8 and 10.0 MPa for test pieces taken axially and transversally from the tubular film. The corresponding time-to-break values were 120 and 100 sec. The creep test was interrupted at a certain moment, the surroundings of the crack were fixed in a clamp, and the crack was photographed both in the strained and relaxed states.

The micrographs of test pieces cut in the machine and cross directions are shown in Figs 6 and 7. The left side of each of the series of photographs corresponds to the crack fixed in the stressed state, while the right column of photographs shows the state of the crack after 5 min relaxation. Fig. 8 corresponds to micrograph No. 9 of Fig. 7, but for the case when additional strain strengthening has very effectively blocked the crack propagation. The barrier of strain strengthened material can be seen predominantly in the lower part of Fig. 8, which demonstrates the crack in the relaxed state. The crack root remains extended also in the relaxed state because of the permanent plastic deformation in this region; it has even split into two separated tips which suggests two possible directions of further crack propagation.

Measurements of the micrographs in Figs 6 and 7 made possible the plot of the time dependence of characteristic crack dimensions, i.e. of the length c and of the crack opening ϕ (maximal crack width at the edge of the test piece). The time dependence curves of these quantities are shown in Fig. 9, along with the creep curves. The numbered points on the creep curves correspond to the similarly numbered photographs in Figs 6 and 7. Similar to the microphotographs, graphs on the left side correpond to test pieces cut in the machine direction, while those on the right side correspond to test pieces taken in the cross-direction. The curves corresponding to the crack in the stressed state are solid, those corresponding to the released crack are broken.

The graphs in Fig. 9 show clearly that the kinetics of crack propagation is distinctly affected by orientation of the material. In test pieces taken in the cross direction, the crack is stable at the beginning and grows only insignificantly; in this region, crack opening is reversible to a great extent, thus being determined only by deformation of the film near the crack. At a later stage crack propagation accelerates, and a considerable part of the crack opening increment remains even after the test piece has been released. The behaviour of test pieces in the machine direction is complementary to some extent: the crack starts growing immediately after stress application, after which its development is slowed down, and only in the last catastrophic stage of the process does the rate of crack propagation steeply increase once again. Consequently, the time dependence curve of the crack opening is S-shaped, also in the case of a released crack. In this case the higher ϕ (crack opening) values are caused by the higher stress used, and hence by the higher overall strain at any given moment. In the range of crack propagation examined (to some 10% of the test piece width), the permanent component of the crack opening ϕ (of the overall crack opening ϕ) is larger for test pieces in the machine direction ($\sim$ 50%) compared with those in the cross direction ($\sim$ 30%). In most cases, especially for a well developed crack, the

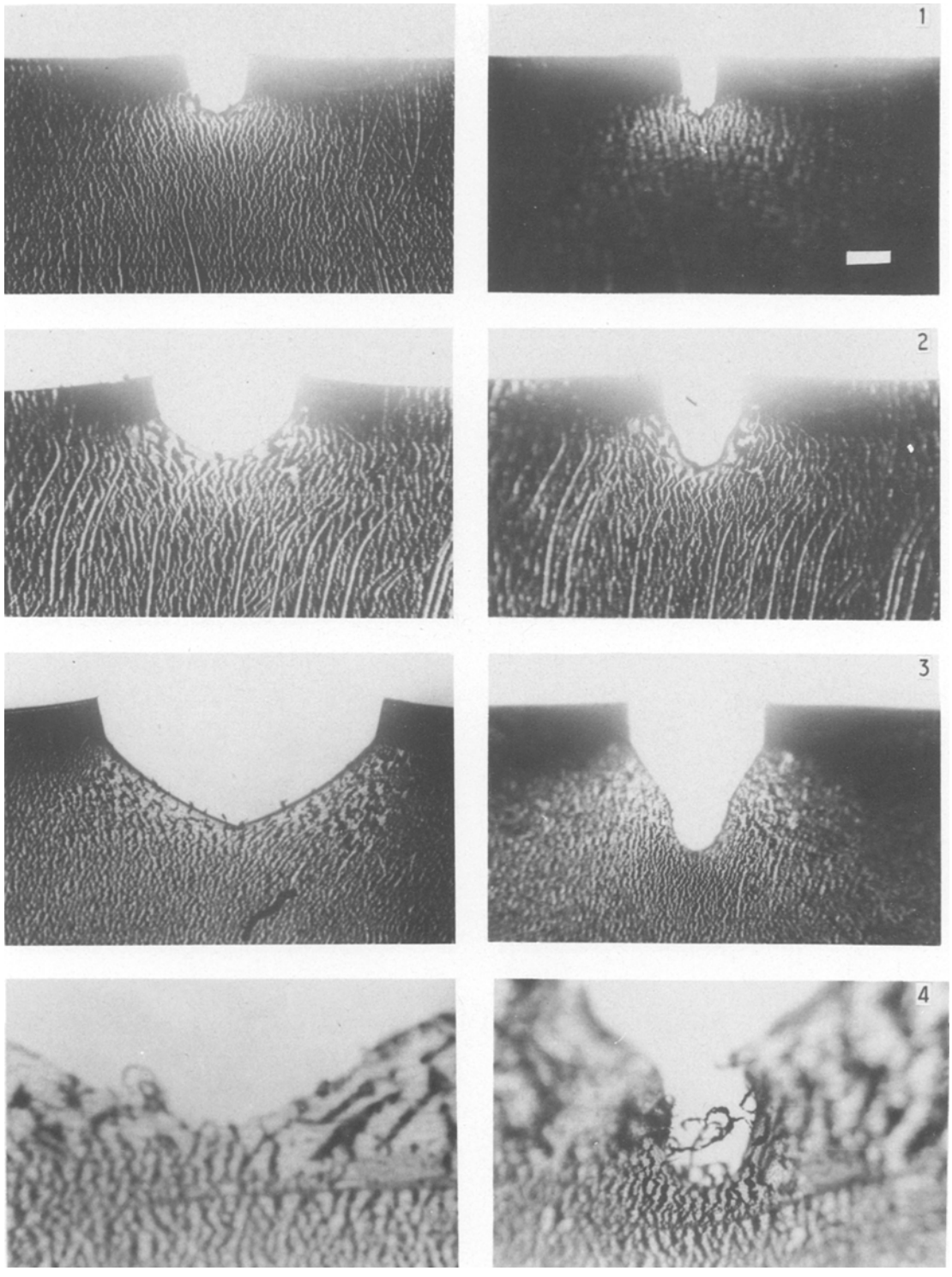

Figure 6 Micrographs of various stages of crack propagation, initial length $c_0 = 0.2$ mm, during the creep test of test pieces in the machine direction with a vacuum-deposited aluminium layer. Micrographs on the left side show the crack in the stressed state, micrographs in the right column correspond to the state 5 min after release. (Initial incision length $c_0 = 0.2$ mm, initial stress $\sigma = 14.8$ MPa. The number of the micrographs corresponds to similarly numbered points of the creep curve in Fig. 9a, left side.) Bar = 0.2 mm.

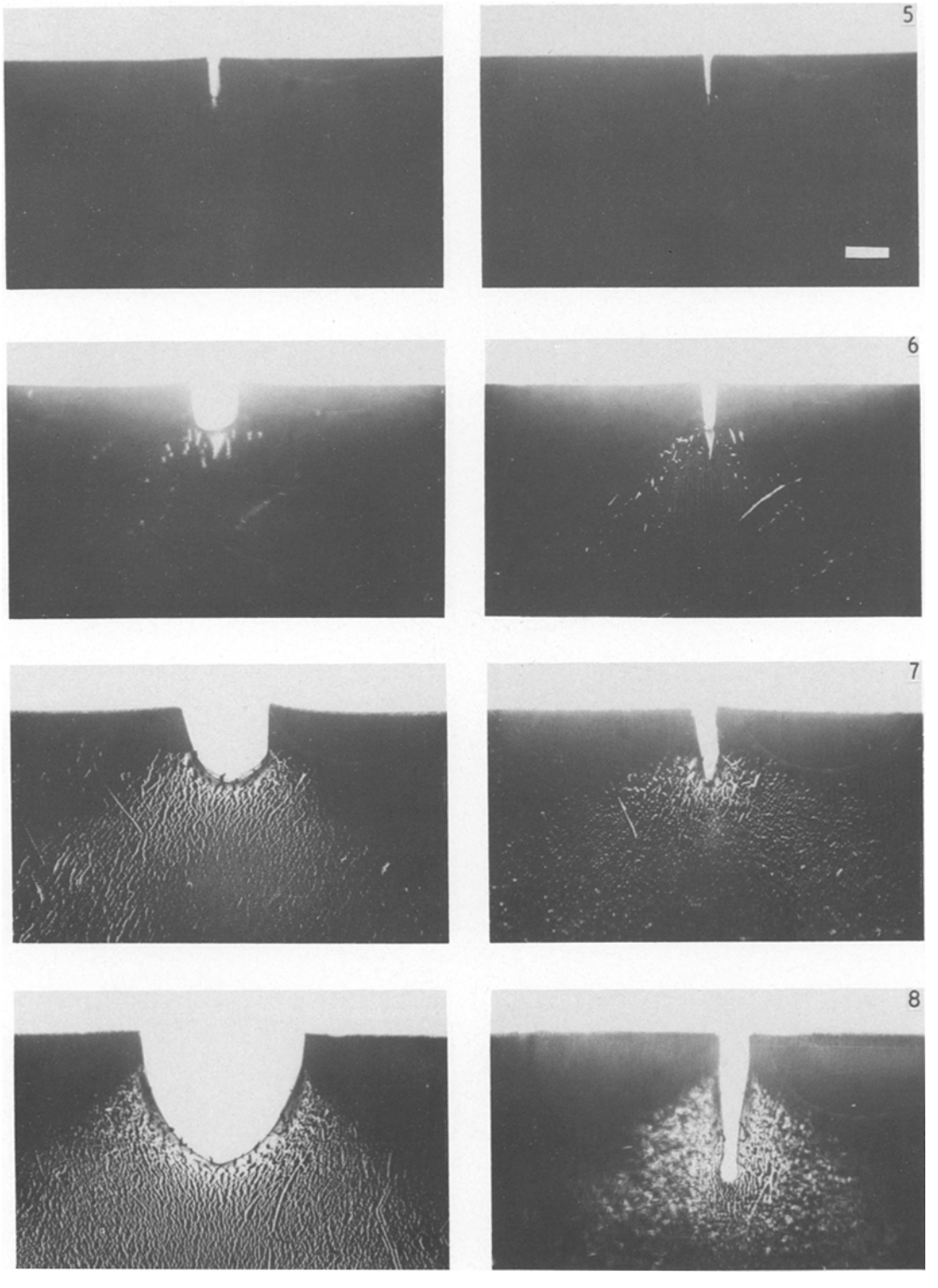

Figure 7 Micrographs of various stages of crack propagation, during the creep test of test pieces in the cross direction with a vacuum-deposited aluminium layer. Left side shows the crack in the stressed state and the right side is 5 min after release. (Initial incision length $c_0 = 0.2$ mm, $\sigma = 10$ MPa. The number of the micrographs corresponds to similarly numbered points of the creep curve in Fig. 6a, right side.) Bar = 0.2 mm.

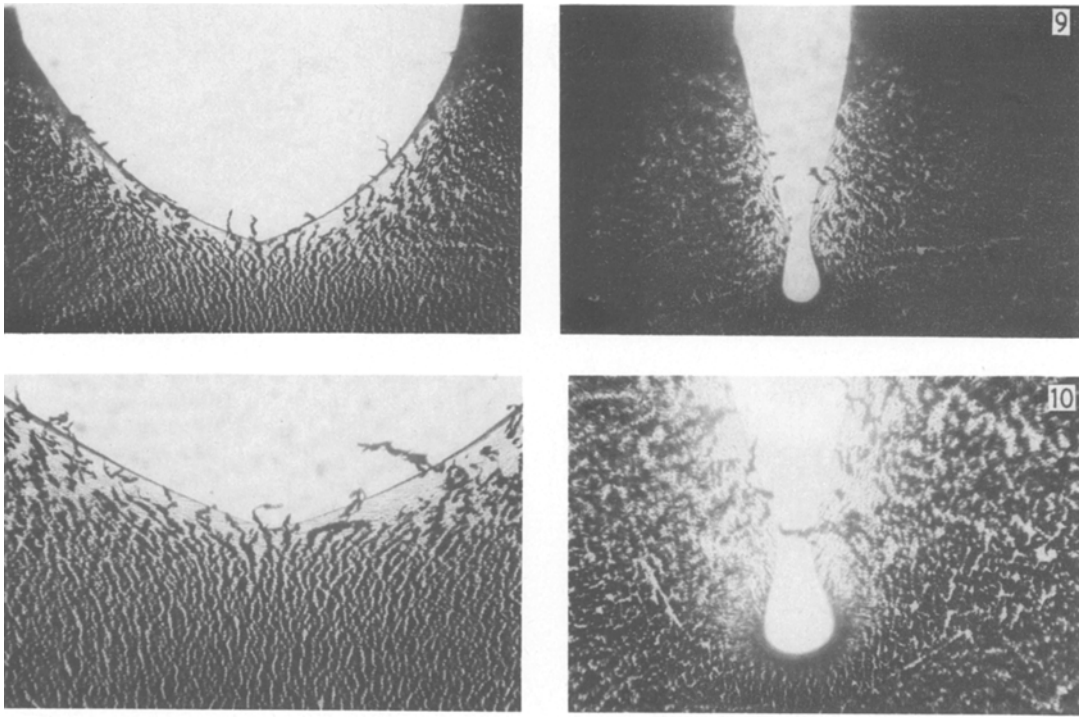

Figure 7 Continued.

crack length measured perpendicular to the axis of the test piece is larger in the released state than that obtained for the stressed crack. This is due to a contraction of the test piece and a resulting decrease in the angle between the crack sides. The largest tangential stress along the periphery of the elliptic crack lies just in its root. Hence, permanent plastic deformation, which remains after the crack has been released, develops first at the root of the crack, while deformation of the material nearer to the edge of the test piece may still be reversible. The crack after release has then a shape resembling a half dumb-bell, as demonstrated, e.g. by the micrographs in Fig. 7. The shape of the crack also depends on the dynamic situation. While a static crack develops to an elliptic shape, the tip of the propagating crack is wedge-shaped.

It is noteworthy that the introduction of a microscopic incision into the film changes the order of strain-at-break values in both main directions: the test pieces with artificial cracks exhibit a higher strain-at-break in the machine direction than in the cross direction, which is behaviour opposite to that of (initially) flaw-free specimens

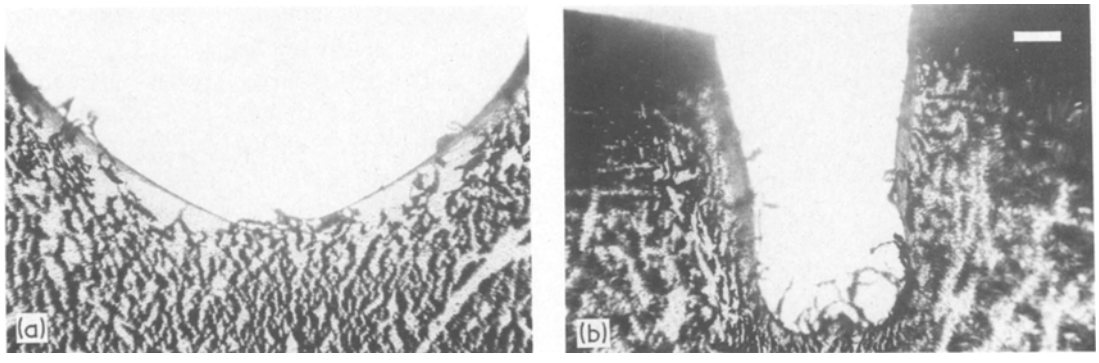

Figure 8 Micrograph of a crack, (a) fixed in the stressed state, (b) 5 minutes after release, of initial length $c_0 = 0.2$ mm, in a test piece taken in the cross direction, 90 sec after application of stress $\sigma = 10$ MPa. The micrograph shows the case of an additional strain strengthening and blunting of the crack peak. Bar = 0.1 mm.

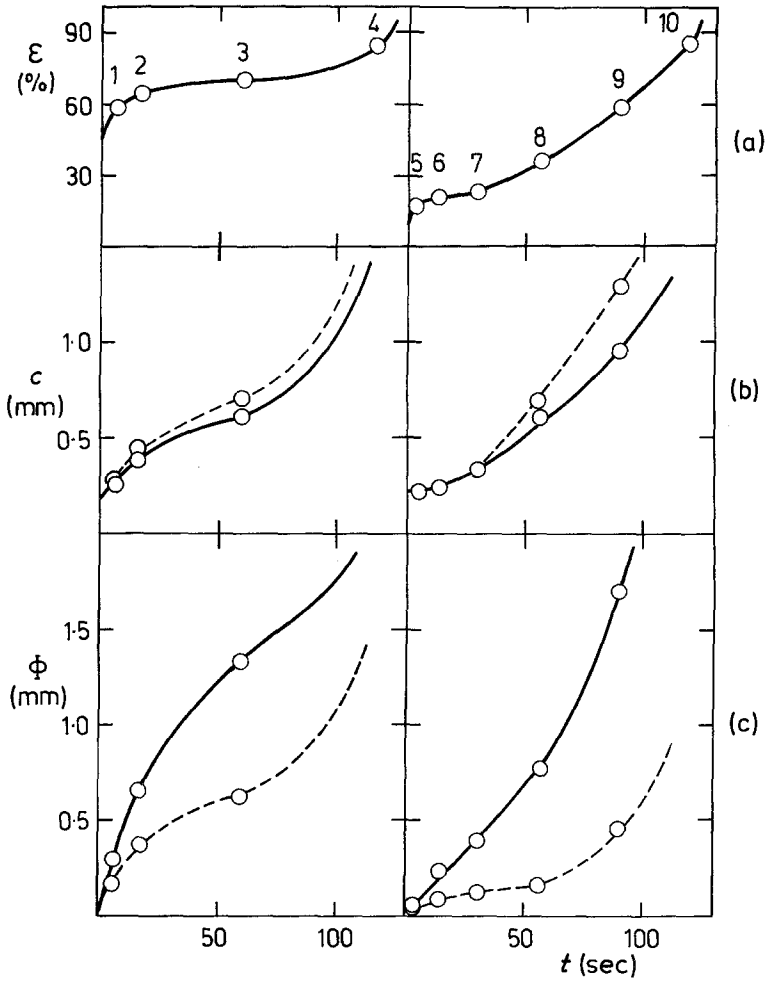

Figure 9 Kinetics of crack propagation in the creep test. The left side shows test pieces in the machine direction and the right side shows test pieces in the cross direction. The solid curves show the crack in the stressed state and the broken curves are 5 min after release of the crack. (a) Average course of the creep curves. (Points numbered as in the micrograph in Fig. 6.) (b) Time dependence of crack length c. (c) Time dependence of crack opening ϕ.

without macroscopic defects. The relationship between the length c of a crack growing from the initially introduced incision and the external macroscopic strain ϵ measured at the clamps of the creep apparatus is demonstrated in Fig. 10. The crack is more stable, if its axis is perpendicular to the direction of prevailing orientation (i.e. for a test piece cut in the machine direction). However, after crack initiation the dependence $c = c(\epsilon)$ is much steeper in this case than that observed for test pieces taken in the cross direction.

3.2. Crack propagation at constant strain rate

While in the creep test the time dependence of overall strain is an experimental function of external load and material, in the tensile test on the tensile testing machine the constant strain rate is the input signal and the force is a dependent variable. This is also the cause underlying the different kinetics of crack propagation in both different loading regimes, even if the stress geometry is the same in both cases.

The dependence of the notch length c, measured with a comparator at various stages of the tensile test, on external deformation ϵ, is represented by the solid lines in Fig. 11, for two initial crack sizes ($c_0 = 0.2$ and 1.0 mm) and for test pieces in the machine and cross directions. The corresponding stress–strain curves are represented with broken lines. As can be seen, the incision starts growing only after the macroscopic yield point has been reached, then is accelerated until complete failure of the test piece is reached. Similarly to the creep test, the crack is more stable in test pieces cut in the machine direction. For example, in the case of the initial notch size $c_0 = 0.2$ mm the crack propagation does not become faster under an external strain of some 45%, while for samples in the cross direction the initiation of the crack begins at 25% overall strain. These critical strain values are of course lower at a larger initial crack. Thus, a more

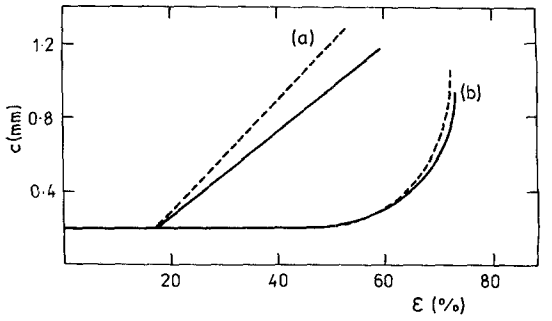

Figure 10 Dependence of crack length c on total external strain for test pieces in (a) the cross and (b) the machine directions. The solid line shows the crack in the stressed state and the broken line is the released crack.

efficient blocking of a crack is reflected macroscopically in a higher strain-at-break value.

The largest crack length which could still be estimated visually was about 20 to 30% of the overall width of the test piece, at a moment immediately before the final fast breaking of the test piece. This corresponds to the second local maximum on the stress–strain curve. If the tensile test machine stops beyond this point, crack propagation continues spontaneously and in an unstable manner until complete failure of the sample. For this reason, the respective crack length c_D may be regarded as critical at the given stress. Of course, the behaviour of the polyethylene film cannot be described in terms of linear fracture mechanics. In spite of this, however, we tried to characterize the film toughness in both main directions by a value $K_D = \sigma(\pi c_D)^{1/2}$, formally analogous to the fracture toughness K_{IC}. The values of the tentative quantity K_D for data in Fig. 11 have been summarized in Table I. Without any requirements as to general validity or comparison with other materials, this table convincingly demonstrates the higher film toughness along the machine direction.

Applying von Mises' criterion, Narisawa *et al.* [8] derived the following expression for the elastic–plastic contour ahead of the crack tip

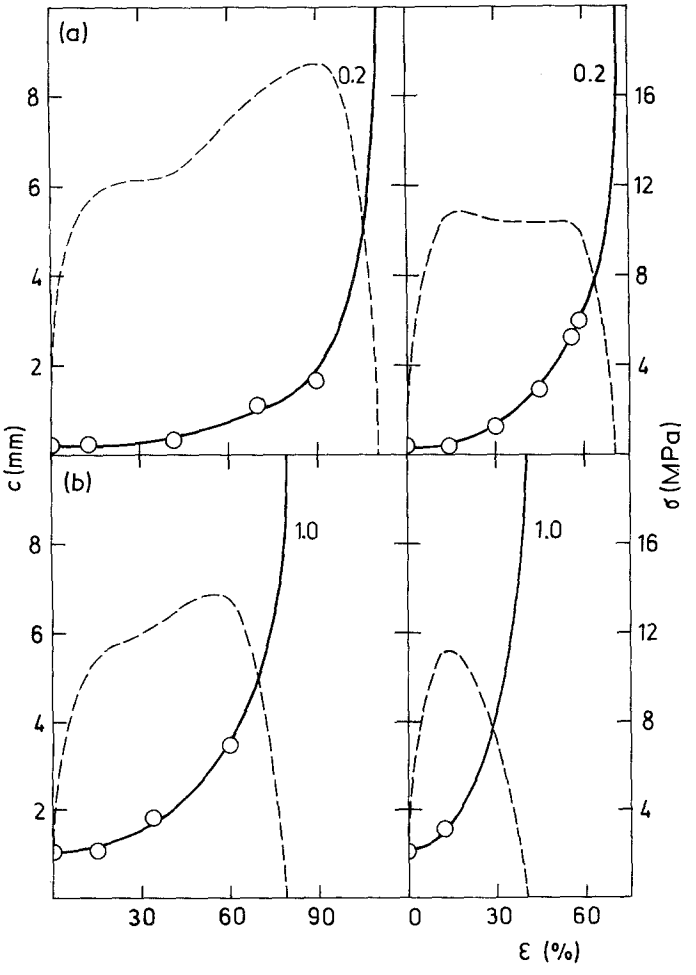

Figure 11 Dependence of crack length c on macroscopic strain (solid curves) in a tensile test at a constant strain rate together with the corresponding stress–strain curves (broken curves). The crack lengths are: (a) $c_0 = 0.2$ mm, (b) $c_0 = 1.00$ mm; the left side shows test pieces in the machine direction and the right side shows test pieces in cross direction.

TABLE I Tentative values of the characteristics of toughness $K_D = \sigma(\pi c_D)^{1/2}$ for test pieces cut in the machine direction (MD) and in the cross direction (CD)

Test piece	c_0 (mm)	K_D ($\times 10^{-6}$ Nm$^{-3/2}$)
MD	0.2	1.92
	1.0	1.98
CD	0.2	1.37
	1.0	1.10

$$\mathbf{r} = (\sigma^2 \pi c / 2\sigma_y^2) \cos^2 [(\theta/2)(1 + 3 \sin \theta/2)], \quad (1)$$

where $\mathbf{r}$ is the radius vector of the contour of the plastic region, θ is the angle between this vector and the crack axis, σ is stress, σ_y is the yield stress, c is the crack length and the origin of the polar coordinate system is situated at the tip of the crack. The equation indicates a heart-shaped plastic region around the crack root. We followed the approach of Narisawa *et al.* [8] and calculated the $\mathbf{r}$ values in the direction of the axis of the crack ($\theta = 0$) for various subsequent stages of its development. The results obained from simultaneously measured σ and ϵ values are summarized in Table II. For the final unstable stage of the crack propagation one can see that the region of plastic deformation virtually encompasses the whole width of the test piece.

A comparison between the crack development in the creep experiment and in the constant strain rate regime shows that at a given external deformation and with a given initial crack size, the instantaneous crack length is larger in the second test type. In other words, at a given instantaneous magnitude of the defect (and also at the moment of the break of the test piece), external macroscopic strain as measured by the Instron tester is smaller than in the creep experiments. This result reflects the time-dependent strain of the film beyond the crack region.

3.3. Strain topography of the crack surroundings

The distribution of local strains has been examined in greater detail for crack No. 7 of Fig. 7, developed from the initial incision having a length $c_0 = 0.2$ mm in a test piece taken in the cross direction. These samples showed an anomalous maximum on the time-to-break–stress curve. The region around the crack was fixed 30 sec after a stress $\sigma = 10$ MPa was applied. Local strain was determined from the cracked thin aluminium layer which was vacuum deposited prior to deformation [5, 6], and evaluated on a micrograph of the crack surroundings photographed in the transmitted light. The region under investigation was divided into uniform square fields on a micrograph magnified 128 x. In each field, strain was detemined five times along the mutually-shifted straight lines parallel to the external stress, and an average was calculated from the results in each square. The local elongation $\lambda = l/l_0 = (\epsilon + 1)$ along one straight line was determined as the ratio of the length of one side of the basic square ($l = 1$ cm) to the sum of the widths of strips of the metal layer (l_0). This procedure was repeated approximately sixty times in the crack surroundings. After that, the particular fields of the rectangular network were connected into regions corresponding to a certain strain interval. The strain map of the crack surroundings thus obtained is shown in Fig. 12, both for a crack fixed in the stressed rate and for the released state. Fig. 12 also shows that regions of a certain strain remain basically unchanged even after the stress had been released, but become smaller as it corresponds to the overall contraction of the region surrounding the crack. The smallest strain values (2 to 5%) are of course reversible to a great extent, which could not be reflected in the method employed. Once

TABLE II Dimensions of the plastic zone r (mm) in the direction of crack axis ($\theta = 0$) according to Equation 1 [8] for various sizes of introduced crack c_0 and various values of overall strain ϵ of the test piece

ϵ (%)	Machine direction		Cross direction	
	$c_0 = 0.2$ mm	$c_0 = 1.0$ mm	$c_0 = 0.2$ mm	$c_0 = 1.0$ mm
5	0.15	0.83	0.17	0.96
15	0.31	1.73	0.31	2.55
30	0.54	2.81	0.89	–
45	0.89	5.09	2.18	–
60	1.82	8.42	4.20	–
75	3.76	–	–	–
90	5.82	–	–	–

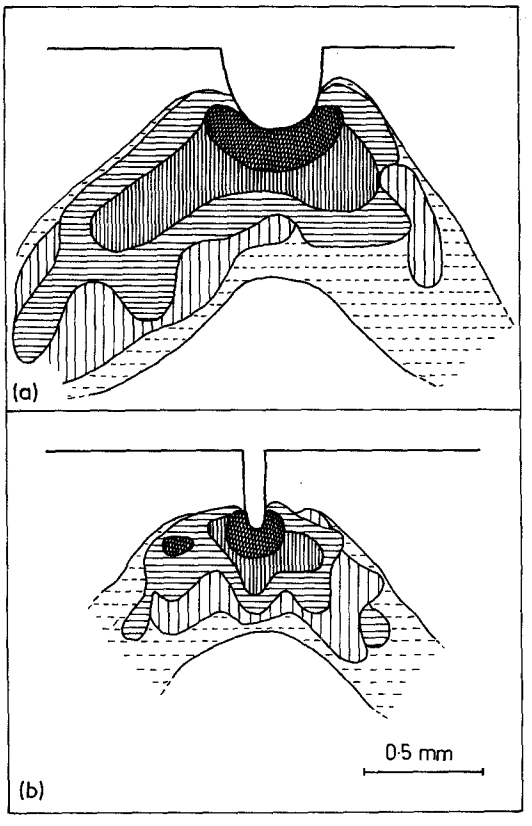

Figure 12 Topography of strain field in the surroundings of the propagating crack, initial length $c_0 = 0.2$ mm, test piece taken in cross direction 30 sec after application of stress, $\sigma = 10$ MPa (the same conditions as for crack No. 7 of Fig. 7). (a) Crack fixed in stressed state and (b) released crack.

cracked, the metal layer transmits light in the crack sites even after release. The light diffraction and scattering extend the respective light traces on the photographic layer. Consequently, the smallest strain values obtained in the released state are unrealistic. The strain field around the crack is approximately symmetrical along the crack axis with the exception of a small shift of some regions towards the left part of the diagram (this may reflect the actual properties of the film or be caused by an improper clamping of the sample).

The whole strained region (with the exception of the largest strains above 40%) is situated along two bands which form an angle of approximately 45° with the crack axis, i.e. along lines with the highest shear stress. The method used in the evaluation of local strains is sensitive, however, mainly to the tensile stress component, in this case in the direction of the axis of the test strip. This controversy may be explained by assuming that the shear stress initiated the onset of plastic deformation, which was then further developed along the tensile stress component.

Equation 1 gives a different shape of the plastically deformed region. In the direction of the crack axis ($\theta = 0$) it predicts plastic deformation up to the distance $\mathbf{r} = \sigma^2\pi c/2\sigma_y^2$. The yield point $\sigma_y = 10.5$ MPa was read off from the stress–strain trace for a test rate of 1 cm min^{-1} approximately corresponding to the average rate of the creep test at 10 MPa. After substitution into Equation 1, we have $\mathbf{r} = 0.498$ mm ~ 0.5 mm. The boundary of the 10% strain region lies just at this distance from the crack peak. Macroscopic strain at the yield point determined experimentally by the tensile test is approximately 16%, which is a fair agreement. For the highest strain values, the shape of the strained region also approximately corresponds to that of the plastically deformed zone, given by Equation 1. On the contrary, regions of strain below the yield point are situated rather along the lines of the highest shear stress, as already mentioned. A similar shape of the strained region near an artificially introduced crack in a polycarbonate film was ascertained by Narisawa *et al.* [8], who photographed test pieces under load in polarized light.

It is this kidney-shaped region of the highest strains ahead of the crack tip which acts as the assumed barrier preventing further propagation of fracture processes in the film. Hence, this zone of orientation-strengthened material is the structural reason underlying a secondary lag on the creep curves [4], and also a maximum on the time-at-break–stress curves. The crack arrest at an oriented region in a test piece cut in the cross direction is illustrated by the photograph in Fig. 8. The crack had an initial length of 0.2 mm and propagated for 90 sec under a constant external stress of 10 MPa. The crack surroundings were then photographed under a microscope in the fixed and released states. The photographs show that the crack propagation along its axis was stopped by the barrier of plastic deformation and the crack began to develop in the directions of the maximal shear stress upwards and downwards. In a crack with its tip thus blunted, the hindering effect of the plastic zone is supplemented by the geometrical effect of

the extended crack front, which distributes the fracture processes into the bulk of the material.

The actual microstructural and geometrical situation at the crack root is of course a result of random processes affected by many parameters. This is why the efficiency of crack blocking differs for different test pieces, or is only slight (if, e.g. due to structural inhomogeneity the crack continuously circumvents the plastic zone already formed). Macroscopically, these random processes are reflected in a large scatter of time-to-break, especially in the region of the maximum.

4. Conclusion

Critical conditions for the crack instability in the test piece follow from the classical Griffith theory [9]. Even though this concept was a very important stimulus for the development of fracture mechanics, in its original form it is unsatisfactory for most of the real materials. The reason should be seen, on the one hand, in the too low value of characteristic energy in the Griffith relation, and on the other, in the time dependence of the fracture process. It is the time phenomena that cause crack propagation in a stressed polymeric film to pass through at least two points of instability: the first of them corresponds to the onset of a slow "subcritical" growth, while the second (of the Griffith type) corresponds to the onset of the fast catastrophic crack propagation. The slow stage of the subcritical crack propagation may moreover be interrupted by a lag due to the orientational strengthening of material surrounding the crack tip. As suggested by experimental results presented in this study, the latter phenomena are the casue underlying the occurrence of a maximum on the time-to-break–stress dependence in a polyethylene film, and probably also in other materials capable of orientational strengthening.

Acknowledgements

We are indebted to Ing. Gerth Jonsson, AB Celloplast, Norrköping, Sweden, and Dr Arne Holmström, Swedish National Authority for Testing, Inspection and Metrology, Borås, Sweden, for kindly supplying the polyethylene film and its basic characteristics. We also wish to thank Mr J. Tauchman, Institute of Macromolecular Chemistry, Prague, for technical assistance.

References

1. M. RAAB and F. LEDNICKÝ, *Zeitschr. Angew. Mathem. Mech.* **48** (1968) T 155.
2. M. RAAB, *J. Macromol. Sci.-Phys.* **B5** (1971) 285.
3. M. RAAB, Z. PELZBAUER, J. JANÁČEK and M. ŠTOL, *J. Polymer Sci.* **C38** (1972) 221.
4. M. RAAB and G. IVANOVA, *Int. J. Fract.* **15** (1979) R 107.
5. Z. PELZBAUER, Proceedings of the 9th All-Union Conference on Electron Microscopy, Tbilisi, October 1973, (Academy of Sciences of the USSR, Moscow, 1973) p. 71.
6. F. LEDNICKÝ and Z. PELZBAUER, Proceedings of the 15th Czechoslovakian Conference on Electron Microscopy, Prague, August 1977 (Czechoslovak Academy of Sciences, Prague, 1977) Vol. B, p. 561.
7. E. H. ANDREWS, "Fracture in Polymers" (Oliver and Boyd, Edinburgh and London, 1968) p. 151.
8. I. NARISAWA, M. ISHIKAWA and H. OGAWA, *Polymer J.* **8 (2)** (1976) 181.
9. A. A. GRIFFITH, *Phil. Trans. Roy. Soc.* **A221** (1921) 163.

Received 9 April and accepted 20 May 1981.